ACS SENSORS

Letter

Cite This: ACS Sens. 2018, 3, 569−573

pubs.acs.org/acssensors

Carbon Nanotube Formic Acid Sensors Using a Nickel Bis(*ortho*-diiminosemiquinonate) Selector

Sibo Lin and Timothy M. Swager*

Department of Chemistry and the Institute for Soldier Nanotechnologies, Massachusetts Institute of Technology, Cambridge, Massachusetts 02139, United States

Supporting Information

ABSTRACT: Formic acid is corrosive, and a sensitive and selective sensor could be useful in industrial, medical, and environmental settings. We present a chemiresistor for detection of formic acid composed of single-walled carbon nanotubes (CNTs) and nickel bis(*ortho*-diiminosemiquinonate) (**1**), a planar metal complex that can act as a ditopic hydrogen-bonding selector. Formic acid is detected in concentrations as low as 83 ppb. The resistance of the material decreases on exposure to formic acid, but slightly increases on exposure to acetic acid. We propose that **1** assists in partial protonation of the CNT by formic acid, but the response toward acetic acid is dominated by inter-CNT swelling. This technology establishes CNT-based chemiresistive discrimination between formic and acetic acid vapors.

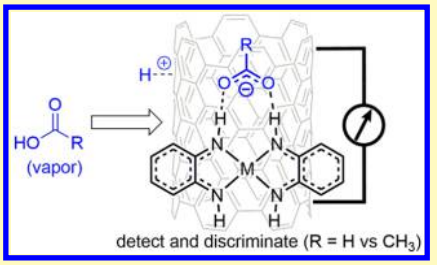

KEYWORDS: *formic acid, carbon nanotubes, chemiresistor, nickel, gas sensor*

Formic acid, the simplest organic acid, is highly pungent and corrosive with a Permissible Exposure Limit (U.S. OSHA PEL) of 5 ppm. An inexpensive, real-time, electronic sensor for formic acid vapors can protect worker health and limit formicary corrosion of metal components.[1] Formic acid sensors can also be useful in diagnosing health conditions,[2−4] monitoring air quality,[5−7] tracking the spread of invasive formicine ant species such as *Nylanderia fulva* ("tawny crazy ant"),[8] and enabling automated pest control. Sensors would facilitate the adoption of formic acid as a hydrogen carrier for energy storage.[9] While much work has been done on low-power aqueous-phase pH sensors,[10−13] *volatile* acidity detectors have been less explored. A selective formic acid detector should be able to discriminate it from other polar compounds. For example, formic and acetic acid are present in similar quantities in environmental and human breath samples, and their discrimination has utility.[2,14]

Carbon nanotube (CNT)-based chemiresistors are an attractive platform for developing gas sensors. Although colormetric[15−17] and metal-oxide and -nitride chemiresistors[18] for formic acid detection exist, CNT chemiresistors are cost-effective, low-power, and operational at room temperature.[19−21] CNT chemiresistors can be straightforwardly integrated with electronic devices, making them ideal candidates for distributed sensor networks.[22,23] While strong acids have been shown to protonate and p-dope CNTs (Figure 1a),[22,24−27] there have been few reports of the chemiresistive response of CNTs to carboxylic acids. Specifically, vertically aligned CNT arrays have a chemi*capacitive* response to formic acid.[28] Chemical-vapor-deposition-grown graphene becomes more conductive upon exposure to acetic acid vapor.[29] A single-CNT field effect transistor (FET) responds to propanoic acid vapors upon functionalization with guanine-rich single-stranded DNA.[30]

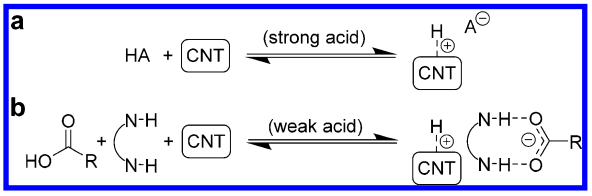

Figure 1. Carbon nanotube protonation and p-doping by (a) strong acid or (b) carboxylic acid assisted by anion receptor.

However, these device architectures require greater manufacturing and operating complexity than chemiresistors based on solution-processed networks of CNTs. Networks of covalently modified CNTs have been reported to increase in resistance, nonselectively, on exposure to acetic acid or other volatile organics via a swelling mechanism.[31,32] Studies on CNT-based vapor sensors discriminating between formic and other carboxylic acids are lacking.

We have investigated planar ditopic complexes as selectors to improve the sensitivity and selectivity of CNT-based sensors toward formic acid. We hypothesized that selectors bearing ditopic hydrogen-bond donors could promote protonation of CNTs by carboxylic acids by stabilizing the carboxylate anion (Figure 1b). Looking to Nature's formate dehydrogenase for selector inspiration, the highly conserved Arg587 residue is known to be crucial in formate binding as a ditopic hydrogen bond donor.[33] Structurally related ureas/thioureas are receptors for carboxylates.[34−36] For CNT-based chemiresistors, previous work has shown that thioureas can act as effective selectors for

Received: January 10, 2018
Accepted: February 14, 2018
Published: February 16, 2018

DOI: 10.1021/acssensors.8b00026
ACS Sens. 2018, 3, 569−573

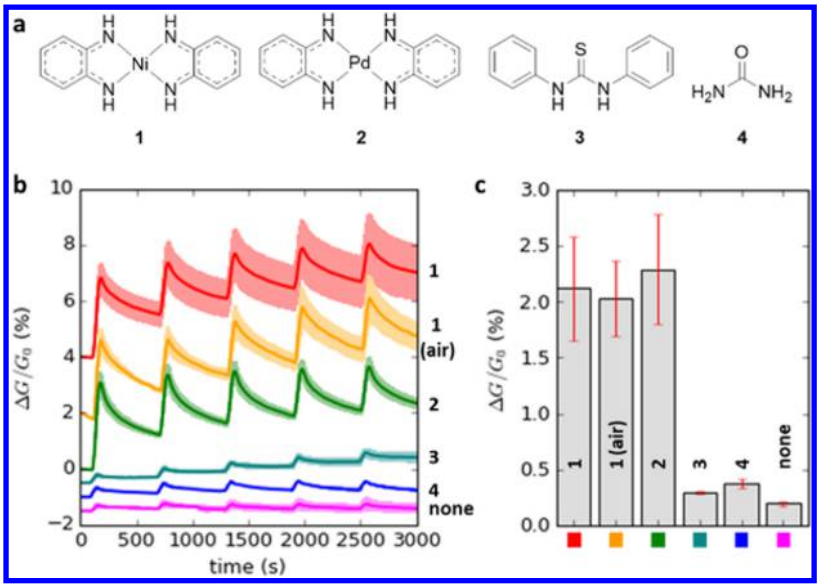

Figure 2. Formic acid vapor sensing (37 ppm) with CNT chemiresistors and (a) molecular selectors. (b) Each trace (vertically offset for clarity) is the average of four sensors with the standard deviation illustrated in a lighter shade; five cycles of 1 min exposure and 9 min purge. The carrier gas is N_2 unless otherwise noted. (c) Average conductivity change for each selector. Error bars represent one standard devation across 20 data points (five measurements each across four devices).

cyclohexanone, and the *N*-aryl substituents are key to tranducing a chemiresistive response to CNTs through noncovalent $\pi-\pi$ interactions.[37,38]

In this study, we used square planar complexes **1** and **2** (Figure 2a)[39] as selectors. The N−H moieties can participate in ditopic H-bonding with carboxylate,[40] while the molecular planarity should enhance electronic communication though $\pi-\pi$ interactions.[41,42] Adding 0−4 equiv of tetrabutylammonium acetate to **1** in d^6-dimethyl sulfoxide (DMSO) results in a distinct shift of the N−H protons from 8.8 to 9.2 ppm (see Supporting Information, Figure S2). This behavior is consistent with competitive H-bonding to acetate and DMSO. UV−vis−NIR absorption spectra of **1** in *N*,*N*-dimethylformamide (DMF) solution show a marked decrease in the LLCT band at 784 nm after exposure to CNTs, indicating strong CNT adsorption of **1** (Figure S7).

Chemiresistors made from CNT networks noncovalently functionalized with selector were exposed to formic acid at 37 ppm in N_2 at room temperature (2% of its saturated vapor pressure from a calibrated oven held at 40 °C). Analyte exposures were set at 1 min followed by a 9 min purge. Devices made with **1** or **2** exhibited semireversible 2% increases in conductivity, whereas devices made with *N*,*N*′-diphenylthiourea (**3**), urea (**4**), or no selector increased conductivity less than 0.4% (Figure 2b). Because benchtop DMF solutions of **1** remained stable for weeks while those of **2** formed brown particulate, further sensing experiments were conducted with **1** as the selector. An experiment using air (35% relative humidity) as the carrier gas instead of N_2 for CNT/**1** sensors gave a similar response.

We then demonstrated the sensitivity of CNT/**1** chemiresistors to formic acid (Figure 3a). The response is linear over nearly 3 orders of magnitude. This dynamic range includes the industrially relevant OSHA PEL of 5 ppm. The experimental limit of detection, 83 ppb, could conceivably be lowered by using longer exposure times.

We established the selectivity of CNT/**1** chemiresistors by exposure to a variety of other volatile organic compounds at 2%

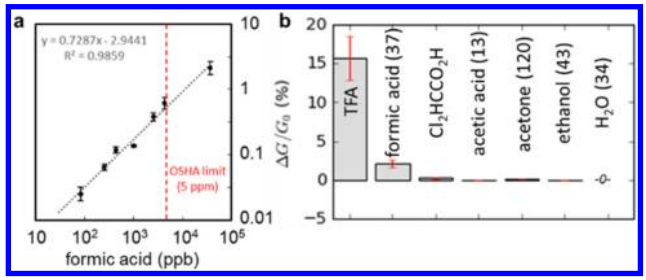

Figure 3. Average conductivity change (N = 20) of CNT/**1** upon 1 min exposures to (a) a range of formic acid concentrations and (b) various analytes at 2% of their saturated vapor from 40 °C analyte oven. For calibrated analytes, concentrations are listed parenthetically (ppm).

of their saturated vapor pressure from a 40 °C analyte oven (Figure 3b). Trifluoroacetic acid (TFA), dichloroacetic acid, and acetone induced increases in conductivity per exposure of 16%, 0.23%, and 0.15%. Acetic acid and ethanol resulted in small decreases in conductivity (−0.05% and −0.07%). Water did not cause any change in conductivity. The strong conductivity increase upon TFA exposure correlates with the high acidity of TFA (pK_a = 0.0). Dichloroacetic acid, while a strong acid (pK_a = 1.25), has lower volatility and thus a relatively low conductivity increase. Acetic acid is less acidic than formic acid (pK_a = 4.75 vs 3.75), and the chemiresistive *decrease* in conductivity is consistent with swelling of inter-CNT gaps, similar to the responses observed for ethanol in this study. Acetic acid vapor also decreased conductivity in previous CNT network chemiresistive sensors.[31,32] As a result, this sensor is selective for formic acid and stronger acids over acetic acid. This selectivity (and reversibility of the response) make CNT/**1** chemiresistors unique from sensors based on strong Brønsted bases, which would be irreversible and not distinguish between various carboxylic acids.[5,15]

To interrogate the mechanism of this chemiresistive response, CNT/**1** was examined with Raman spectroscopy (Figure S8). While the weak CNT D-band (~1340 cm^{-1}) is

DOI: 10.1021/acssensors.8b00026
ACS Sens. 2018, 3, 569−573

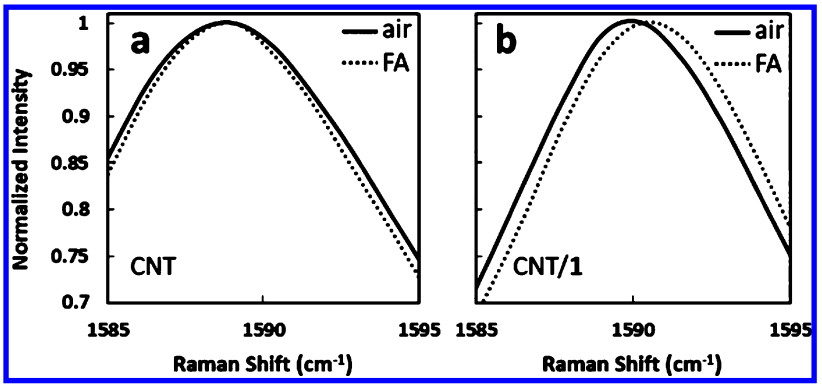

Figure 4. Raman G-band of (a) CNT and (b) CNT/**1** under under ambient air or air saturated with formic acid vapor (FA).

obscured by overlapping signals from **1**, the CNT G-band is distinct near 1590 cm^{-1} under ambient air. Under saturated formic acid vapor, however, the G-band shifts to higher energy by 0.5 cm^{-1} (Figure 4b). Other sharp Raman features of CNT/**1** are not similarly shifted (Figure S9). Based on previous studies of CNTs in acidic solution,[24,43] this shift corresponds to an introduction of approximately one hole per 640 carbon atoms in the CNT sample upon formic acid vapor exposure. Identical measurements of a sample of CNT without **1** showed no shift in the G-band (1589 cm^{-1}) under ambient air or formic acid vapor (Figure 4a). These Raman observations are consistent with **1** facilitating protonation and p-doping of the CNTs.

To investigate the effect of π-stacking between the CNT and **1**, we turned to computational models. Although **1** has nontrivial electronic structure as a result of ligand-based radical character, previous studies have shown accurate modeling using density function theory (DFT).[44,45] Thus, a segment of (6,6)-CNT and **1** were geometry-optimized using a two-layer ONIOM scheme in which **1** and the nearest C_{24} fragment (coronene) of the CNT were treated with restricted-spin, dispersion-corrected DFT while the remaining CNT atoms were modeled semiempirically. In the resulting structure, the metal complex adopts the curvature of the underlying CNT (Figure 5a). Furthermore, the short distance between the N atoms of the metal complex and the nearest CNT atoms (3.22 Å) supports a $\pi-\pi$ interaction. The electronic structure was then examined via a single-point calculation, treating the whole model with DFT. The resulting density-of-states (DOS) plot shows a Fermi level of −5.94 eV compared to −5.99 eV for bare (6,6)-CNT (Figure 5c). Thus, **1** donates partial electron density to the CNT, activating the CNT toward protonation with mild acids. For comparison, an analogous model of (6,6)-CNT/**3** also showed short nonbonded N−C contacts (Figure 5b), but the Fermi level shifts the opposite direction to −6.00 eV, indicating very slight withdrawal of electron density from the CNT. These results corroborate the experimental observation that CNT/**1** chemiresistors respond to formic acid more readily than CNT or CNT/**3** sensors.

In summary, square-planar metal complex selectors **1** and **2** leverage their chelating N−H moieties to facilitate protonation/p-doping of the CNT chemiresistor network by formic acid vapors. The resulting simple, low-power CNT/**1** sensors can detect formic acid at concentrations relevant to industrial settings with short 1 min exposure times. Although there is cross-reactivity with stronger acids, there is notably a smaller (and inverted) response to acetic acid, establishing the first CNT-based chemiresistive discrimination between formic and acetic acid vapors. Computational models also show that **1** can effectively π-stack and donate partial electron density into the CNT network. We are interested in extending the use of **1**, **2**, and related metal complexes as selectors to detect and discriminate isosteres of carboxylate such as bicarbonate, phosphate, and arsenate in aqueous solution.

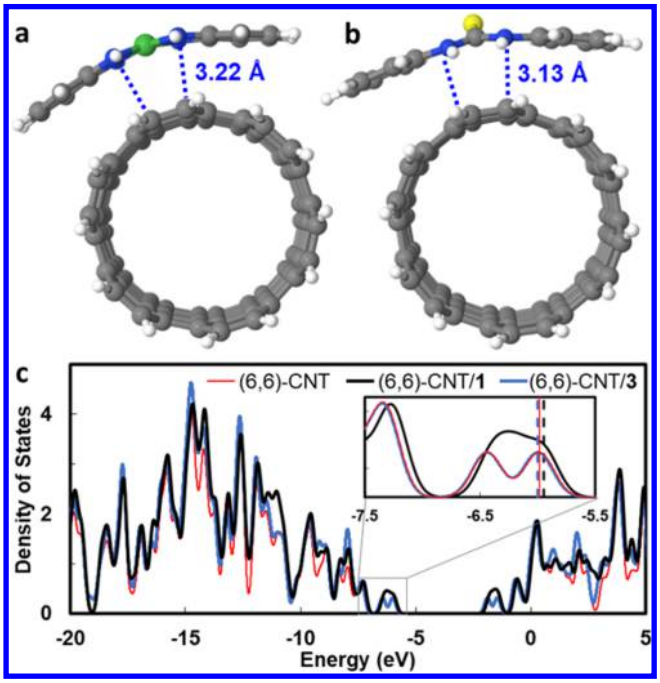

Figure 5. (a) Structural models of (6,6)-CNT/**1** and (b) (6,6)-CNT/**3**. (c) DOS plots of (6,6)-CNT with and without **1** or **3**. Inset: magnified view of frontier states with Fermi levels indicated by vertical lines.

■ ASSOCIATED CONTENT

Supporting Information

The Supporting Information is available free of charge on the ACS Publications website at DOI: 10.1021/acssensors.8b00026.

Spectroscopic characterization, computational details (PDF)

■ AUTHOR INFORMATION

Corresponding Author

*E-mail: tswager@mit.edu.

DOI: 10.1021/acssensors.8b00026
ACS Sens. 2018, 3, 569−573

ORCID

Sibo Lin: 0000-0001-5922-6694
Timothy M. Swager: 0000-0002-3577-0510

Notes

The authors declare no competing financial interest.

■ ACKNOWLEDGMENTS

This work was supported by the Army Research Office through the use of facilities at the Institute for Soldier Nanotechnologies and National Science Foundation, DMR-1410718. S.L. was supported by NIH F32 NRSA (# GM110897).

■ REFERENCES

(1) Mikhailov, A. A. Effect of Low-Molecular Carbon Acids on Atmospheric Corrosion of Metals. *Prot. Met. Phys. Chem. Surf.* **2009**, *45* (7), 757−765.
(2) Greenwald, R.; Johnson, B. A.; Hoskins, A.; Dworski, R. Exhaled Breath Condensate Formate after Inhaled Allergen Provocation in Atopic Asthmatics *In Vivo*. *J. Asthma* **2013**, *50* (6), 619−622.
(3) Greenwald, R.; Fitzpatrick, A. M.; Gaston, B.; Marozkina, N. V.; Erzurum, S.; Teague, W. G. Breath Formate Is a Marker of Airway S-Nitrosothiol Depletion in Severe Asthma. *PLoS One* **2010**, *5* (7), e11919.
(4) McMartin, K. E.; Ambre, J. J.; Tephly, T. R. Methanol Poisoning in Human Subjects. Role for Formic Acid Accumulation in the Metabolic Acidosis. *Am. J. Med.* **1980**, *68* (3), 414−418.
(5) Yan, Y.; Lu, D.; Zhou, H.; Hou, H.; Zhang, T.; Wu, L.; Cai, L. Polyaniline-Modified Quartz Crystal Microbalance Sensor for Detection of Formic Acid Gas. *Water, Air, Soil Pollut.* **2012**, *223* (3), 1275−1280.
(6) Nielsen, G. D.; Hansen, L. F.; Andersen, B.; Poulsen, N. Indoor Air Guideline Levels for Formic, Acetic, Propionic and Butyric Acid. *Indoor Air* **1998**, *8* (S5), 8−24.
(7) Stavrakou, T.; Müller, J.-F.; Peeters, J.; Razavi, A.; Clarisse, L.; Clerbaux, C.; Coheur, P.-F.; Hurtmans, D.; De Mazière, M.; Vigouroux, C.; et al. Satellite Evidence for a Large Source of Formic Acid from Boreal and Tropical Forests. *Nat. Geosci.* **2011**, *5* (1), 26−30.
(8) Wang, Z.; Moshman, L.; Kraus, E.; Wilson, B.; Acharya, N.; Diaz, R. A Review of the Tawny Crazy Ant, Nylanderia Fulva, an Emergent Ant Invader in the Southern United States: Is Biological Control a Feasible Management Option? *Insects* **2016**, *7* (4), 77.
(9) Sordakis, K.; Tang, C.; Vogt, L. K.; Junge, H.; Dyson, P. J.; Beller, M.; Laurenczy, G. Homogeneous Catalysis for Sustainable Hydrogen Storage in Formic Acid and Alcohols. *Chem. Rev.* **2018**, *118*, 372.
(10) Besteman, K.; Lee, J. O.; Wiertz, F. G. M.; Heering, H. A.; Dekker, C. Enzyme-Coated Carbon Nanotubes as Single-Molecule Biosensors. *Nano Lett.* **2003**, *3* (6), 727−730.
(11) Fu, Q.; Liu, J. Integrated Single-Walled Carbon Nanotube/microfluidic Devices for the Study of the Sensing Mechanism of Nanotube Sensors. *J. Phys. Chem. B* **2005**, *109* (28), 13406−13408.
(12) Li, C. A.; Han, K. N.; Pham, X.-H.; Seong, G. H. A Single-Walled Carbon Nanotube Thin Film-Based pH-Sensing Microfluidic Chip. *Analyst* **2014**, *139* (8), 2011.
(13) Gou, P.; Kraut, N. D.; Feigel, I. M.; Bai, H.; Morgan, G. J.; Chen, Y.; Tang, Y.; Bocan, K.; Stachel, J.; Berger, L.; et al. Carbon Nanotube Chemiresistor for Wireless pH Sensing. *Sci. Rep.* **2015**, *4* (1), 4468.
(14) Khare, P.; Kumar, N.; Kumari, K. M.; Srivastava, S. S. Atmospheric Formic and Acetic Acids: An Overview. *Rev. Geophys.* **1999**, *37* (2), 227−248.
(15) Sensidyne Industrial Health & Safety Information. Formic Acid 1−50 ppm Gas Detector Tube; http://www.sensidyne.com/colorimetric-gas-detector-tubes/detector-tubes/216s-formic-acid.php (accessed Nov 21, 2017).
(16) Grant, W. M. Colorimetric Microdetermination of Formic Acid Based on Reduction to Formaldehyde. *Anal. Chem.* **1948**, *20* (3), 267−269.
(17) Genovese, M. E.; Colusso, E.; Colombo, M.; Martucci, A.; Athanassiou, A.; Fragouli, D. Acidochromic Fibrous Polymer Composites for Rapid Gas Detection. *J. Mater. Chem. A* **2017**, *5* (1), 339−348.
(18) Eckshtain-Levi, M.; Capua, E.; Paltiel, Y.; Naaman, R. Hybrid Sensor Based on AlGaN/GaN Molecular Controlled Device. *ACS Sensors* **2016**, *1* (2), 185−189.
(19) Schnorr, J. M.; Swager, T. M. Emerging Applications of Carbon Nanotubes. *Chem. Mater.* **2011**, *23*, 646−657.
(20) Snow, E. S.; Perkins, F. K.; Robinson, J. A. Chemical Vapor Detection Using Single-Walled Carbon Nanotubes. *Chem. Soc. Rev.* **2006**, *35* (9), 790.
(21) Kauffman, D. R.; Star, A. Carbon Nanotube Gas and Vapor Sensors. *Angew. Chem., Int. Ed.* **2008**, *47* (35), 6550−6570.
(22) Ishihara, S.; Labuta, J.; Nakanishi, T.; Tanaka, T.; Kataura, H. Amperometric Detection of Sub-Ppm Formaldehyde Using Single-Walled Carbon Nanotubes and Hydroxylamines: A Referenced Chemiresistive System. *ACS Sensors* **2017**, *2* (10), 1405−1409.
(23) Zhu, R.; Azzarelli, J. M.; Swager, T. M. Wireless Hazard Badges to Detect Nerve-Agent Simulants. *Angew. Chem., Int. Ed.* **2016**, *55* (33), 9662−9666.
(24) Parra-Vasquez, A. N. G.; Behabtu, N.; Green, M. J.; Pint, C. L.; Young, C. C.; Schmidt, J.; Kesselman, E.; Goyal, A.; Ajayan, P. M.; Cohen, Y.; et al. Spontaneous Dissolution of Ultralong Single- and Multiwalled Carbon Nanotubes. *ACS Nano* **2010**, *4* (7), 3969−3978.
(25) Davis, V. A.; Parra-Vasquez, A. N. G.; Green, M. J.; Rai, P. K.; Behabtu, N.; Prieto, V.; Booker, R. D.; Schmidt, J.; Kesselman, E.; Zhou, W.; et al. True Solutions of Single-Walled Carbon Nanotubes for Assembly into Macroscopic Materials. *Nat. Nanotechnol.* **2009**, *4* (12), 830−834.
(26) Strano, M. S.; Huffman, C. B.; Moore, V. C.; O'Connell, M. J.; Haroz, E. H.; Hubbard, J.; Miller, M.; Rialon, K.; Kittrell, C.; Ramesh, S.; et al. Reversible, Band-Gap-Selective Protonation of Single-Walled Carbon Nanotubes in Solution. *J. Phys. Chem. B* **2003**, *107* (29), 6979−6985.
(27) Puech, P.; Hu, T.; Sapelkin, A.; Gerber, I.; Tishkova, V.; Pavlenko, E.; Levine, B.; Flahaut, E.; Bacsa, W. Charge Transfer between Carbon Nanotubes and Sulfuric Acid as Determined by Raman Spectroscopy. *Phys. Rev. B: Condens. Matter Mater. Phys.* **2012**, *85* (20), 205412.
(28) Chen, Y.; Meng, F.; Li, M.; Liu, J. Novel Capacitive Sensor: Fabrication from Carbon Nanotube Arrays and Sensing Property Characterization. *Sens. Actuators, B* **2009**, *140* (2), 396−401.
(29) Nallon, E. C.; Schnee, V. P.; Bright, C.; Polcha, M. P.; Li, Q. Chemical Discrimination with an Unmodified Graphene Chemical Sensor. *ACS Sensors* **2016**, *1* (1), 26−31.
(30) Staii, C.; Johnson, A. T.; Chen, M.; Gelperin, A. DNA-Decorated Carbon Nanotubes for Chemical Sensing. *Nano Lett.* **2005**, *5* (9), 1774−1778.
(31) Niu, L.; Luo, Y.; Li, Z. A Highly Selective Chemical Gas Sensor Based on Functionalization of Multi-Walled Carbon Nanotubes with Poly(ethylene Glycol). *Sens. Actuators, B* **2007**, *126* (2), 361−367.
(32) Hines, D.; Rümmeli, M. H.; Adebimpe, D.; Akins, D. L. High-Yield Photolytic Generation of Brominated Single-Walled Carbon Nanotubes and Their Application for Gas Sensing. *Chem. Commun.* **2014**, *50* (78), 11568−11571.
(33) Hartmann, T.; Schrapers, P.; Utesch, T.; Nimtz, M.; Rippers, Y.; Dau, H.; Mroginski, M. A.; Haumann, M.; Leimkühler, S. The Molybdenum Active Site of Formate Dehydrogenase Is Capable of Catalyzing C−H Bond Cleavage and Oxygen Atom Transfer Reactions. *Biochemistry* **2016**, *55* (16), 2381−2389.
(34) Kelly, T. R.; Kim, M. H. Relative Binding Affinity of Carboxylate and Its Isosteres: Nitro, Phosphate, Phosphonate, Sulfonate, and δ-Lactone. *J. Am. Chem. Soc.* **1994**, *116* (16), 7072−7080.
(35) Hughes, M. P.; Shang, M.; Smith, B. D. High Affinity Carboxylate Binding Using Neutral Urea-Based Receptors with

DOI: 10.1021/acssensors.8b00026
ACS Sens. 2018, 3, 569−573

Internal Lewis Acid Coordination. *J. Org. Chem.* **1996**, *61* (14), 4510−4511.
(36) Fan, E.; Van Arman, S. A.; Kincaid, S.; Hamilton, A. D. Molecular Recognition: Hydrogen-Bonding Receptors That Function in Highly Competitive Solvents. *J. Am. Chem. Soc.* **1993**, *115* (1), 369−370.
(37) Schnorr, J. M.; van der Zwaag, D.; Walish, J. J.; Weizmann, Y.; Swager, T. M. Sensory Arrays of Covalently Functionalized Single-Walled Carbon Nanotubes for Explosive Detection. *Adv. Funct. Mater.* **2013**, *23* (42), 5285−5291.
(38) Frazier, K. M.; Swager, T. M. Robust Cyclohexanone Selective Chemiresistors Based on Single-Walled Carbon Nanotubes. *Anal. Chem.* **2013**, *85* (15), 7154−7158.
(39) Balch, A. L.; Holm, R. H. Complete Electron-Transfer Series of the [M-N $_4$] Type. *J. Am. Chem. Soc.* **1966**, *88* (22), 5201−5209.
(40) Bill, E.; Bothe, E.; Chaudhuri, P.; Chlopek, K.; Herebian, D.; Kokatam, S.; Ray, K.; Weyhermüller, T.; Neese, F.; Wieghardt, K. Molecular and Electronic Structure of Four- and Five-Coordinate Cobalt Complexes Containing Two *O* -Phenylenediamine- or Two *O* -Aminophenol-Type Ligands at Various Oxidation Levels: An Experimental, Density Functional, and Correlated Ab Initio Study. *Chem. - Eur. J.* **2005**, *11* (1), 204−224.
(41) Georgakilas, V.; Tiwari, J. N.; Kemp, K. C.; Perman, J. A.; Bourlinos, A. B.; Kim, K. S.; Zboril, R. Noncovalent Functionalization of Graphene and Graphene Oxide for Energy Materials, Biosensing, Catalytic, and Biomedical Applications. *Chem. Rev.* **2016**, *116* (9), 5464−5519.
(42) Noro, S. I.; Chang, H. C.; Takenobu, T.; Murayama, Y.; Kanbara, T.; Aoyama, T.; Sassa, T.; Wada, T.; Tanaka, D.; Kitagawa, S.; et al. Metal-Organic Thin-Film Transistor (MOTFT) Based on a Bis(o-Diiminobenzosemiquinonate) nickel(II) Complex. *J. Am. Chem. Soc.* **2005**, *127* (28), 10012−10013.
(43) Sumanasekera, G. U.; Allen, J. L.; Fang, S. L.; Loper, A. L.; Rao, A. M.; Eklund, P. C. Electrochemical Oxidation of Single Wall Carbon Nanotube Bundles in Sulfuric Acid. *J. Phys. Chem. B* **1999**, *103* (21), 4292−4297.
(44) Bachler, V.; Olbrich, G.; Neese, F.; Wieghardt, K. Theoretical Evidence for the Singlet Diradical Character of Square Planar Nickel Complexes Containing Two O-Semiquinonato Type Ligands. *Inorg. Chem.* **2002**, *41* (16), 4179−4193.
(45) Herebian, D.; Wieghardt, K. E.; Neese, F. Analysis and Interpretation of Metal-Radical Coupling in a Series of Square Planar Nickel Complexes: Correlated Ab Initio and Density Functional Investigation of [Ni(LISQ)2] (LISQ = 3,5-Di-Tert-Butyl-O-Diimino-benzosemiquinonate (1-)). *J. Am. Chem. Soc.* **2003**, *125* (36), 10997−11005.

DOI: 10.1021/acssensors.8b00026
ACS Sens. 2018, 3, 569−573